

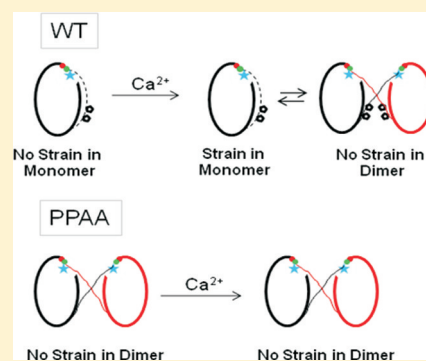
# Prolines in $\beta$ A-Sheet of Neural Cadherin Act as a Switch To Control the Dynamics of the Equilibrium between Monomer and Dimer

Nagamani Vunnam and Susan Pedigo\*

Department of Chemistry and Biochemistry, University of Mississippi, University, Mississippi 38677, United States

**S** Supporting Information

**ABSTRACT:** Neural cadherins dimerize through the formation of calcium-dependent strand-crossover structures. Dimerization of cadherins leads to cell–cell adhesion in multicellular organisms. Strand-crossover dimer forms exclusively between the first N-terminal extracellular modules (EC1) of the adhesive partners via swapping of their  $\beta$ A-sheets and docking of tryptophan-2 in the hydrophobic pocket. In the apo-state wild-type cadherin is predominantly monomer, which indicates that the dimerization is energetically unfavorable in the absence of calcium. Addition of calcium favors dimer formation by creating strain in the monomer and lowering the energetic barrier between monomer and dimer. Dynamics of the monomer–dimer equilibrium is vital for plasticity of synapses. Prolines recurrently occur in proteins that form strand-crossover dimer and are believed to be the source of the strain in the monomer. N-cadherins have two proline residues in the  $\beta$ A-sheet. We focused our studies on the role of these two prolines in calcium-dependent dimerization. Spectroscopic, electrophoretic, and chromatographic studies showed that mutations of both prolines to alanines increased the dimerization affinity by  $\sim 20$ -fold and relieved the requirement of calcium in dimerization. The PSA and P6A mutant formed very stable dimers that required denaturation of protein to disassemble in the apo conditions. In summary, the proline residues act as a switch to control the dynamics of the equilibrium between monomer and dimer which is crucial for the plasticity of synapses.



Neural cadherins (N-cadherins) are located at excitatory synapses and play an important role in synaptogenesis, synapse maintenance,<sup>1,2</sup> synaptic plasticity,<sup>3,4</sup> and long-term potentiation.<sup>5</sup> The adhesive interface in the synapse is a strand-crossover structure. The dynamics of this strand-crossover structure is crucial for plasticity of the synapse. Here we report the studies of a proline mutant of N-cadherin that is predominantly dimer regardless of the calcium concentration. Studies of this mutant give insight into the importance of proline in the dynamics of the strand-crossover structure.

The extracellular (EC) region of N-cadherin participates in the formation of strand-crossover dimer.<sup>6</sup> The EC region has five tandemly repeated EC domains (EC1–EC5) with three calcium-binding sites at the interface between adjacent EC domains. A number of studies showed the requirement of calcium in cadherin-mediated cell–cell adhesion.<sup>7–10</sup> Structural studies<sup>11–13</sup> suggest that the binding of calcium ions induces a conformational change in EC1 by undocking the conserved tryptophan-2, W2, from its own hydrophobic pocket and docking it into the hydrophobic pocket of its adhesive partner, which leads to cell–cell adhesion. Identical interactions, hydrophobic and ionic, are formed in both monomeric and dimeric conformations of cadherins. Thus, the strand-crossover structure forms exclusively between EC1 modules of the adhesive partners via swapping of their  $\beta$ A-sheets.

Strand-crossover dimer formation has been projected as a possible mechanism for protein aggregation.<sup>14</sup> Prolines recurrently occur in the interfacial region of proteins that

form strand-crossover dimers. The conformational restrictions of proline side chains are believed to be the source of the strain in the monomeric conformation of proteins,<sup>15</sup> which is relieved upon dimerization. Recent studies have shown that the proline residues can also energetically favor the monomeric conformation.<sup>16</sup> A proposed model for cadherin dimer formation is that calcium binding induces strain in the monomeric conformation that is relieved upon dimer formation.<sup>17</sup> Although different research groups have shown important elements of strand-crossover dimer formation in cadherins, there is very little experimental evidence to explain the thermodynamic details of this process. N-cadherin has two proline residues in the  $\beta$ A-sheet; however, their contribution to strand-crossover formation is not known. Is it because of these proline residues that N-cadherin forms dimer in presence of calcium? Do these proline residues energetically favor the monomer or dimer?

We propose a model for the role of P5 and P6 in the  $\beta$ A-sheet in the formation of strand-crossover dimer by N-cadherin. According to this model, the proline residues are the origin of the calcium dependence of dimerization. On the basis of the discussion above, we predict that mutation of these proline residues will favor the monomer conformation. To investigate this model, we created a protein with the double mutations PSA

**Received:** May 19, 2011

**Revised:** June 30, 2011

**Published:** July 1, 2011



and P6A (PPAA) in the  $\beta$ A-sheet. We expected that PPAA would be monomeric regardless of the calcium concentration. Spectroscopic electrophoretic and chromatographic experiments were used to determine the impact of the PPAA mutation on stability, calcium-binding affinity, and calcium-induced dimerization. These studies showed that the PPAA mutation increased the dimerization affinity by  $\sim 20$ -fold compared to wild-type (WT). PPAA was dimeric irrespective of calcium concentration, which indicates that the mutations relieved the requirement of calcium in dimerization. The PPAA mutant created a high activation energy barrier for dimer disassembly in the apo-state. This energy barrier is lowered by denaturing conditions including temperature and guanidine hydrochloride. These results suggest that the disassembly of dimer in the mutant occurs via the denatured state in apo conditions. These studies imply the prolines in WT stabilize the monomer conformation and make the protein dependent on calcium for dimerization. Although these results are surprising, they gave us a new insight into the contribution of proline residues in the dynamics of the monomer–dimer equilibrium. In summary, the proline residues are not required for dimerization, but they are vital for the dynamics of the equilibrium between monomer and dimer which is crucial for the plasticity of adherens junctions like synapses.

## EXPERIMENTAL PROCEDURES

**Site-Directed Mutagenesis.** The construction of the first two ectodomains (residues 1–221), designated as NCAD12 (NCAD12: EC1, linker 1, EC2, linker 2), was described previously.<sup>18</sup> Point mutations were introduced into the NCAD12 sequence by site-directed mutagenesis by using the Quickchange kit (Stratagene) with the following sense primer, PPAA: 5' CGC GAC TGG GTC ATC GCG GCA ATC AAC TTG CCA G 3'. Point mutations were confirmed by sequencing the resulting plasmids.

**Overexpression and Purification.** Protein overexpression and purification were described previously.<sup>18</sup> Purity of digested proteins, NCAD12 wild-type (WT) and NCAD12-P5AP6A (PPAA), was assessed by SDS-PAGE in 17% polyacrylamide gels. The extinction coefficients were determined experimentally based on the amino acid composition using a molar absorption coefficient of tryptophan and tyrosine residues in the denatured state using the method of Edelhoch.<sup>19</sup> The extinction coefficient at 280 nm for WT was  $17\,700 \pm 500 \text{ M}^{-1} \text{ cm}^{-1}$  and for PPAA was  $17\,400 \pm 240 \text{ M}^{-1} \text{ cm}^{-1}$ . Protein concentrations were determined spectrophotometrically using these extinction coefficients.

**Determination of the Stability by Thermal-Unfolding Studies.** Thermal unfolding of WT and PPAA was monitored with an AVIV 202SF CD spectrometer. Experimental conditions were described previously.<sup>20</sup> To observe the effect of calcium binding, studies were performed at two calcium concentrations, Apo (50  $\mu\text{M}$  EGTA) in 140 mM NaCl, 10 mM HEPES, pH 7.4, and the saturated state with 1 mM added calcium. The thermal-unfolding transitions were fit to the Gibbs–Helmholtz equation with linear native and denatured baselines with adjustable slopes and intercepts as described previously.<sup>21</sup> To ensure that the unfolding transition was reversible, CD signal was monitored as unfolded samples were cooled back to 15 °C. The  $\Delta C_p$  for apo-NCAD12 was determined previously<sup>20</sup> from the Kirchoff plot of the observed

enthalpy of denaturation versus transition temperature and found to be 1 kcal/(mol K).

**Native Gel Electrophoresis.** Native gel electrophoresis was used to determine the size of the protein samples. In the native condition, WT and PPAA mutant have same charge; therefore, they separate based on their size. To analyze the purified protein samples, 10  $\mu\text{L}$  of 55  $\mu\text{M}$  protein sample was mixed with 10  $\mu\text{L}$  of native loading buffer (0.5 M Tris/HCl, pH 6.8, 5% glycerol, 2% bromophenol blue), and 10  $\mu\text{L}$  of this mixture was loaded on the 17% PAGE gel. Gels were electrophoresed at 100 V for 2 h at 4 °C and then stained with coomassie.

**Assembly Studies.** Analytical size exclusion chromatography (SEC) was used to monitor the monomer–dimer ratio in protein stocks. We have used this method successfully to illustrate the calcium dependent monomer–dimer equilibria in epithelial and neural cadherins.<sup>20</sup> SEC was performed with a Superose-12 10/300 GL column (Amersham) using an ÄKTA Purifier HPLC with UV absorbance detection at 280 nm. The mobile phase was 140 mM NaCl, 10 mM HEPES, pH 7.4, with a flow rate of 0.5 mL/min. To observe the effect of calcium on dimerization, calcium was added to the protein stocks but not to the mobile phase. The calibration of SEC column was described previously.<sup>20</sup> We monitored the level of monomer and dimer as the height of the peaks detected at 280 nm.

**Monomer–Dimer Equilibria as a Function of Protein Concentration.** To monitor the monomer–dimer equilibria as a function of protein concentration, protein samples were injected to the SEC column at two different protein concentrations (55 and 7  $\mu\text{M}$ ). First, 30  $\mu\text{L}$  of 55  $\mu\text{M}$  sample was injected to the SEC column, and then the 240  $\mu\text{L}$  of 1 to 8 dilution of 55  $\mu\text{M}$  was injected to the column. Thus, an equal amount of protein was injected regardless of the concentration, and hence the UV absorbance should be same at 280 nm.

**Determination of the Equilibrium Dimer Dissociation Constant.** The fact that PPAA makes stable dimeric species allowed us to expand the chromatographic technique into a quantitative method for determining the equilibrium dissociation constant. The determination of the equilibrium dimer dissociation constant using an SEC method was described previously and yielded the value of  $K_d$  for WT, which was in agreement with the  $K_d$  determined by sedimentation velocity experiments.<sup>20</sup> This experiment was repeated in triplicate. Dilution of protein samples on the column will not affect the level of dimer because it is kinetically trapped and does not dissociate on the column.

**Disassembly of Stable Dimer.** The disassembly of WT and PPAA dimers was determined by heat and chemical denaturant, guanidine hydrochloride (GHCl). To determine the effect of temperature on dimer disassembly, protein samples of WT and PPAA at 55  $\mu\text{M}$  were incubated at different temperatures (37, 45, 55, and 65 °C) for 5–60 min. The amounts of monomer and dimer present before and after heating were measured by analytical SEC. To determine the effect of chemical denaturant on dimer disassembly, dimeric protein samples of WT and PPAA at a concentration of 55  $\mu\text{M}$  were incubated at different GHCl concentrations (2 and 4 M) for 1–48 h. The amounts of monomer and dimer present were then measured by analytical SEC.

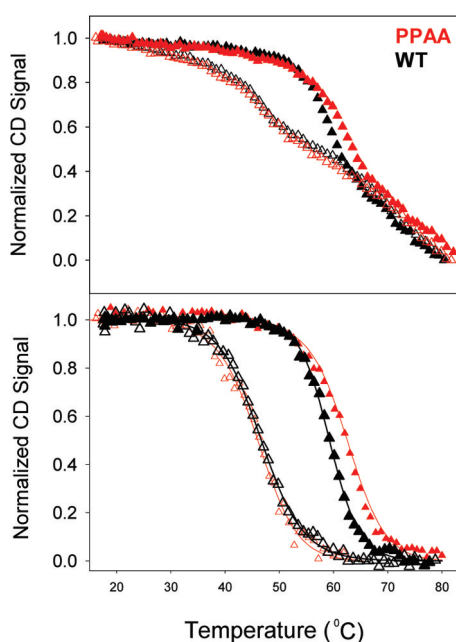


**Figure 1.** Thermal unfolding of WT and PPAA. Thermal unfolding of WT (black) and PPAA (red) at 230 nm. Normalized CD signal versus temperature in the apo ( $\Delta$ ) and 1 mM ( $\blacktriangle$ ) calcium at 5  $\mu$ M protein concentrations. Top panel shows normalized data, and the bottom panel shows the first transition data fitted to the Gibbs–Helmholtz equation and corrected for the fitted baselines. The solid lines are simulated based on resolved parameters.

## RESULTS

**Determination of the Stability by Thermal-Unfolding Studies.** Thermal-unfolding studies were performed to observe the impact of the PPAA mutation on stability. CD spectroscopy was used to monitor structural changes as a function of temperature for WT and PPAA at low protein concentration (5  $\mu$ M) in the absence and presence of calcium. Results from the thermal-unfolding experiments are summarized in Figure 1. Two transitions were observed in both proteins in the apo-state. These two transitions data are in agreement with our previous data from the thermal unfolding of the isolated individual ectodomains, EC1 and EC2. The first transition matches with unfolding of the isolated EC2 ( $T_m$ : 52  $\pm$  6  $^{\circ}$ C; unpublished experiments), and the second transition matches with unfolding of the isolated EC1 ( $T_m$ : 70  $\pm$  4  $^{\circ}$ C; Figure 7, Supporting Information).

**First Transition.** The data from the first transition were fit to a two-state model according to the Gibbs–Helmholtz equation providing estimates for  $T_m$  and  $\Delta H_m$ . In the apo-state WT and PPAA unfolded with similar melting temperatures. However, the mutant showed a decrease in the enthalpy change of unfolding, leading to a decrease in the calculated free energy change at 25  $^{\circ}$ C (Table 1). These results indicate that the PPAA mutations in EC1 decreased the stability of EC2. Both WT and PPAA were stabilized by addition of 1 mM calcium (Figure 1). Although WT and PPAA had similar melting temperatures, the enthalpy of unfolding for PPAA was significantly less than WT. This was reflected as a decreased value for the calculated free energy change for the first transition at 25  $^{\circ}$ C. Since PPAA is less stable than WT in the presence and the absence of calcium, by implication, the proline

**Table 1.** Summary of Parameters Resolved from the First Transition of the Thermal-Unfolding Experiments for WT and PPAA in the Absence and Presence of Calcium

protein	buffer	$\Delta H_m$ (kcal/mol)	$T_m$ ( $^{\circ}$ C)	$\Delta G^{\circ}$ at 25 $^{\circ}$ C (kcal/mol)
WT	Apo	68 $\pm$ 8	45 $\pm$ 2	3.6 $\pm$ 0.5
	Ca <sup>2+</sup>	79 $\pm$ 5	59 $\pm$ 3	6.3 $\pm$ 0.7
PPAA	Apo	55 $\pm$ 5	46 $\pm$ 1	2.9 $\pm$ 0.3
	Ca <sup>2+</sup>	64 $\pm$ 3	62 $\pm$ 1	4.9 $\pm$ 0.2

residues in WT must stabilize the monomeric form of the protein.

**Second Transition.** The primary feature of the second transition is that its position is the same for both proteins and is independent of calcium concentration. Second transition melting temperatures were estimated because of insufficient baseline data. Estimated melting temperatures for WT and PPAA were similar to EC1 melting temperature (Supporting Information). These results indicate that the PPAA mutation did not affect the EC1 structure and stability. Addition of calcium had no impact on second transition of both the proteins, indicating that calcium dissociates before the domain unfolds (Figure 1).

Refolding experiments were performed to test the thermodynamic reversibility of the unfolding transitions. The data from the reversibility experiment showed that PPAA refolds following the unfolding transition (Figure 8A, Supporting Information). The unfolding and refolding transitions of EC1 (second transition) are identical. Denaturation of EC2 is also reversible (first transition), but the refolding transition of EC2 is shifted to a lower  $T_m$  (Figure 8B). This is due to slow kinetics of refolding as supported by the recovery of the CD signal after 4 days of incubation at 4  $^{\circ}$ C (Figure 8C). Analytical SEC results confirmed that heating of the protein does not generate higher molecular weight aggregates (data not shown). These results suggest that protein unfolding is reversible.

In summary, proline mutations in EC1 decreased the stability of EC2, but they do not have any impact on stability of EC1, the domain in which they are located.

**Characterization of Dimeric State of WT and PPAA.** The size of WT and PPAA was determined by analytical SEC. Results are summarized in Figure 2A. WT eluted as two peaks at 12.0  $\pm$  0.1 and 13.1  $\pm$  0.5 mL, and PPAA eluted as single peak at 12.0  $\pm$  0.1 mL. As described elsewhere, these retention volumes represent the dimeric (12.0  $\pm$  0.2 mL) and monomeric (13.0  $\pm$  0.1 mL) species.<sup>20</sup> The dimerization state of these proteins was also confirmed by native gel electrophoresis. The native gel of WT and PPAA showed single bands. PPAA appeared as a condensed band at higher molecular weight, which implies that it is predominantly dimer and it is not in equilibrium with monomer. WT appeared as an extended band, with higher average mobility. These results indicate that the PPAA mutations increased the dimerization affinity such that the form of the protein in the apo-stock was dimeric. The extended band for WT in the native gel represents the monomeric and dimeric forms of the protein, which are in equilibrium.

**Assembly Studies.** Figure 3 represents an outline of experiments that were performed to characterize the different monomeric and dimeric species and the linkage between calcium binding and dimerization equilibria in WT and PPAA. In general, if the monomer and dimer are in equilibrium, their



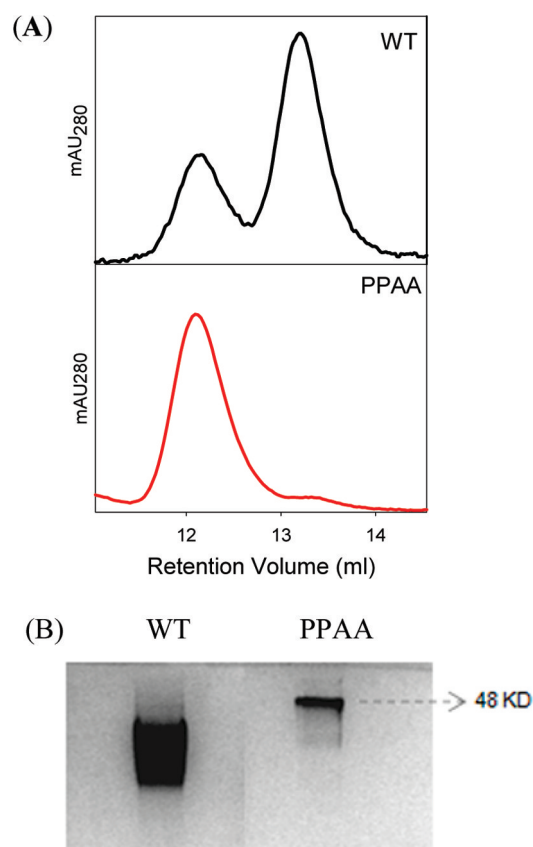


**Figure 2.** Analytical SEC and native gel electrophoresis analysis of WT and PPAA stocks. (A) Top panel shows WT (black, 33% dimer). Bottom panel shows PPAA (red, 98% dimer). (B) Native gel of WT and PPAA.

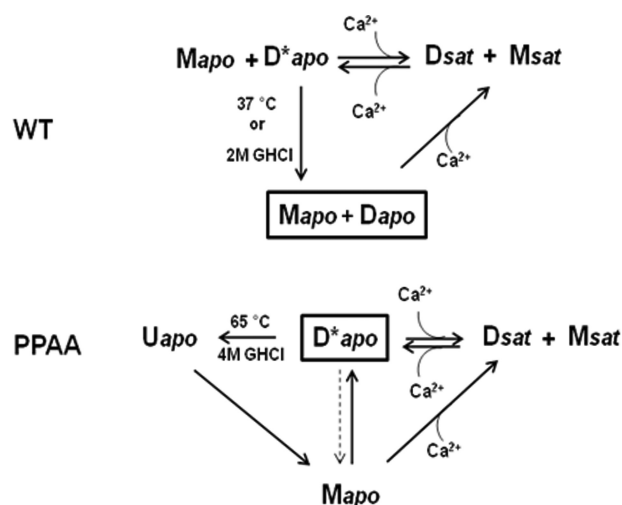


**Figure 3.** A schematic of experiments performed to characterize the different monomeric and dimeric species and the energetic linkage between calcium binding and dimerization equilibria in WT and PPAA.  $M_{apo}$  and  $D_{apo}$  represent the monomeric and dimeric species in the absence of calcium.  $M_{sat}$  and  $D_{sat}$  represent the monomeric and dimeric species in the presence of calcium.  $D^*_{apo}$  represents the stable dimer, and  $U_{apo}$  represents the unfolded protein in the apo-state.

ratio in a solution will be dependent upon the concentrations of protein and calcium. As shown in Figure 2A, the apo-native state of WT is predominantly monomer ( $M_{apo}$ ) and PPAA is

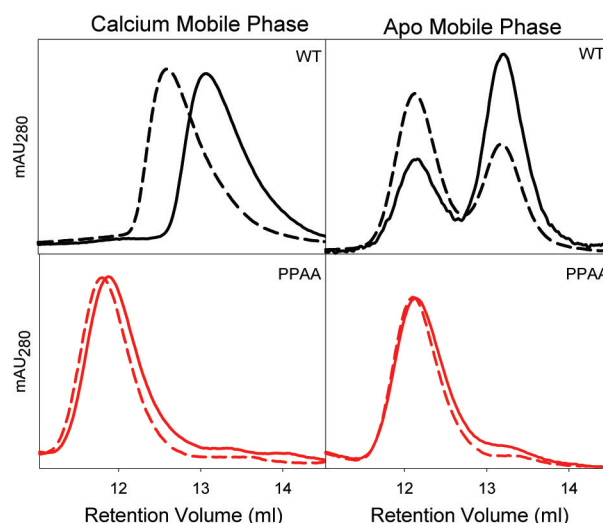


**Figure 4.** Analytical SEC to determine monomer–dimer equilibria as a function of protein and calcium concentrations. Concentrated WT (black) and PPAA (red) stocks (55  $\mu$ M, dashed) were diluted (1:8 to 7  $\mu$ M, solid) in the calcium-bound states (1 mM calcium) to show the effect of protein concentration on the monomer and dimer equilibria. These samples were analyzed in the calcium-saturated conditions (left panels) and in the apo-buffer conditions (right panels).

dimer ( $D^*_{apo}$ ) at 55  $\mu$ M protein concentration as represented by the boxed species in Figure 3. As discussed below analytical SEC experiments were performed as a function of protein and calcium concentration, heat and chemical denaturant (GHCl) in apo and calcium added mobile phases. These studies showed that PPAA mutant forms very stable dimer compared to WT. The evidence for this follows.

**Monomer–Dimer Equilibria as a Function of Protein Concentration.** To monitor the impact of protein concentration on monomer–dimer ratio, analytical SEC experiments were performed on WT and PPAA at two protein concentrations (55 and 7  $\mu$ M) with 1 mM calcium added.

**Apo-Mobile Phase.** Calcium added (1 mM) protein samples at two different protein concentrations, 55 and 7  $\mu$ M, were injected to the SEC column to monitor the change in the level of dimer as a function of protein concentration. Both the proteins eluted as two peaks, which indicates that the monomer–dimer equilibrium is slow in the absence of calcium. Even though protein samples are in the calcium-saturated state, after injecting into the column calcium is depleted from the protein samples. WT had 20% dimer at 7  $\mu$ M and 60% dimer at 55  $\mu$ M protein concentration, indicating that dimerization is coupled with protein concentration (Figure 4). In contrast, PPAA showed 98% dimer at 55 and 7  $\mu$ M protein concentrations (Figure 4). These results suggest that the PPAA increased the dimerization affinity compared to WT.

**Calcium-Mobile Phase.** A similar experiment was performed with calcium added to the mobile phase (1 mM). Protein concentration dependent shifts in retention volumes were observed for WT and PPAA. Both the proteins eluted as single peaks, which indicates that the monomer–dimer equilibrium is rapid in presence of calcium. At high protein concentration, the retention volume moved toward dimer, and at low protein concentration, the retention volume moved toward that of monomer in both WT and PPAA. These results indicate that the monomer–dimer equilibrium is dictated by

protein concentration in presence of calcium. The PPAA mutant had a similar retention volume as dimer, indicating that it has a higher level of dimer compared to WT (Figure 4). The retention volume shift was moderate upon dilution in PPAA compared to WT, which indicates that the PPAA mutant forms very stable dimer (Figure 4). These results confirm that the removal of proline residues from  $\beta$ A-sheet strongly favors the dimerization, thereby implying the presence of these proline residues in WT favors the monomer conformation.

**Determination of the Dissociation Constant.** We performed a series of experiments to determine the equilibrium dissociation constant for dimerization of PPAA. In these experiments, solutions of known protein concentrations (25, 12.5, 6.5, 3, and 2.5  $\mu$ M) and 1 mM calcium concentration were prepared such that there was an equilibrium mixture of monomer and dimer ( $D_{\text{satd}}$ ) as dictated by the protein concentration. EDTA was added, and the calcium stripped from the dimer leading to formation of the kinetically trapped dimer. The level of  $D^*_{\text{apo}}$  was then assayed using the analytical SEC method. This method was used to determine the dissociation constant for WT.<sup>20</sup> Even at 2.5  $\mu$ M of protein concentration PPAA eluted as a dimer (data not shown). From these data, we conclude that PPAA must have a dimerization constant at least 10-fold less than 2.5  $\mu$ M (maximum  $K_d$  is 0.25  $\mu$ M). We performed a similar experiment in the calcium mobile phase in the absence of EDTA similar to experiments shown in Figure 4. We observed the shift in retention volume toward dimer as the protein concentration increased. On the basis of these retention volume shifts, we estimated the  $K_d$  for PPAA ( $\sim 0.1 \mu$ M) since measurements could not be made experimentally at concentrations in the range of nanomolar.

**Disassembly of the Stable Dimer.** Both WT and PPAA forms stable dimer. In WT, the kinetically trapped dimer was formed by stripping the calcium from protein sample,  $D^*_{\text{apo}}$ . PPAA is dimeric in the native state. Heat and GHCl was used to determine the stability of the dimer in these two constructs. WT dimer disassembled at 37  $^{\circ}$ C, and PPAA dimer disassembled at 65  $^{\circ}$ C (Figure 5). These results indicate that the PPAA forms very stable dimer compared to WT. The stability of PPAA dimer was also confirmed by addition of GHCl. WT was disassembled by 2 M GHCl and PPAA was disassembled by 4 M GHCl (Figure 5). These results suggest that the prolines in WT control the dimerization affinity. In summary, our data indicate that the proline residues in the  $\beta$ A-sheet act as an energetic switch to control the dynamics of monomer–dimer equilibrium.

## DISCUSSION

Taken together, our data show that proline residues at the dimer interface in N-cadherin control the dynamics of the monomer–dimer equilibrium, which is crucial for plasticity of the synapse.<sup>3,4,22</sup> On the basis of our studies, we propose a model to demonstrate the role of proline residues in strand-crossover dimerization as represented in Figure 6. In the apo-native state WT is predominantly monomer (depending on protein concentration) and PPAA is dimer. Because of the proline residues in the  $\beta$ A-sheet, WT favors the monomeric conformation in the apo-state, which means that these residues are energetically unfavorable for dimer formation. Our data consistently show that the mutant is dimeric in the apo-native state, supporting this phenomenon. Calcium binding to WT creates strain in the monomeric conformation that is relieved

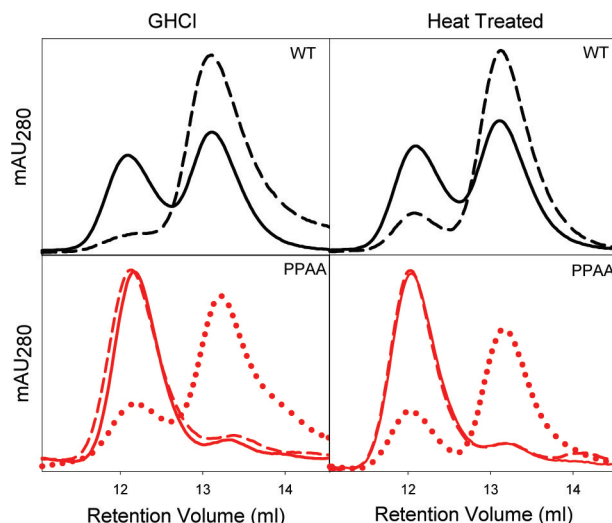


**Figure 5.** Analytical SEC to determine the stability of dimer as a function of temperature and GHCl. Both WT and PPAA proteins were analyzed at 55  $\mu$ M protein concentration. Apo-WT (black) was assayed before (top left panel, solid) and after adding the 2 M GHCl (top left panel, dashed) to monitor the impact of chemical denaturant on dimer disassembly as described in Experimental Procedures. Apo-PPAA (red) was assayed before (bottom left panel, solid) and after adding the 2 M GHCl (bottom left panel, dashed) 4 M (bottom left panel, dotted). Apo-WT (black) was assayed before (top right panel, solid) and after heating for 10 min at 37  $^{\circ}$ C (top right panel, dashed) to monitor the impact of temperature on dimer disassembly. Apo-PPAA (red) was assayed before (bottom right panel, solid) and after heating for 1 h at 37  $^{\circ}$ C (bottom right panel, dashed) and 65  $^{\circ}$ C (bottom right panel, dotted).

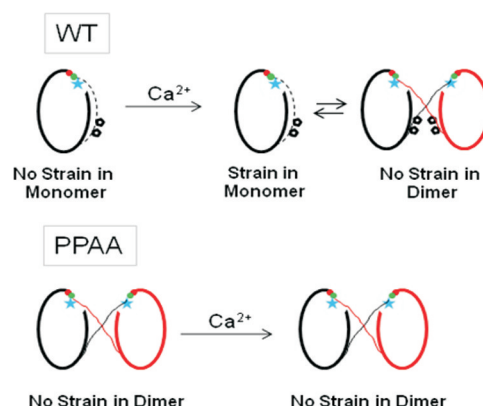


**Figure 6.** A model representing the role of proline residues ( $\bigcirc$ ) at dimer interface. Hydrophobic interaction (blue star) and ionic interaction between E89 (green) and the N-terminus (red) are shown at the dimer interface. The red bubble diagram represents the neighboring cadherin. In the apo-state, WT is predominantly monomeric and PPAA is dimeric. Calcium induces the strain in the monomeric conformation of WT, which leads to dimer formation.

upon dimer formation. Hence, the proline residues confer the calcium requirement for dimerization and also adjust the dimerization affinity. In summary, our data indicate that the proline residues in the  $\beta$ A-sheet act as an energetic switch that controls the dynamics of monomer–dimer equilibrium.

Thermal-unfolding studies were performed to evaluate the impact of the PPAA mutation on the stability of the protein. These studies showed that the PPAA mutations decreased the

stability of EC2 of the protein in the absence and the presence of calcium but did not have any impact on the EC1, where it is located. Studies from our lab have noted the sensitivity of EC2 to its context.<sup>21</sup> The destabilizing effect of EC1 on the stability of EC2 in MECAD12 was also observed in our previous studies.<sup>23</sup> Our current data suggest that the proline residues at dimer interface stabilize the EC2 of wild-type. An alternative explanation is that the dimeric form of PPAA destabilizes EC2. Since the PPAA dimer unfolds at 65 °C, it disassembles as EC1 unfolds, and thus the mutation does not affect the apparent stability of EC1. Our analytical SEC data suggest that the PPAA mutant increased the dimerization affinity and relieved the calcium dependency in dimerization. There is precedence in the literature for this phenomenon. Increase in dimerization affinity upon mutating the proline residues was also observed in other proteins.<sup>16</sup> Our data indicate that conformational restriction due to the side chain of proline residues in WT is energetically unfavorable for dimer formation. To overcome this energetically unfavorable condition, N-cadherin requires calcium binding at the EC1–EC2 interface for dimerization to occur.

In a recent study published while this paper was under review, Vendome et al. used molecular dynamics, sedimentation equilibrium, and X-ray crystallography to address this surprising property of the prolines in the  $\beta$ A-sheet.<sup>24</sup> They found that the single proline mutants, P5A and P6A, as well as the double mutant of ECAD12 formed high-affinity dimers. Their structural studies indicate that there is an increase in the buried hydrophobic surface area at the PPAA dimer interface that creates the high-affinity dimer. We observed a significant difference in the stability of the WT and PPAA dimers. WT disassembled after only 10 min at 37 °C, whereas PPAA required 1 h at 65 °C (Figure 5). Thus, these structural studies support the thermodynamic studies presented here.

The dynamic property of synapses is critical for neural plasticity and synapse remodeling.<sup>25</sup> Our data imply that the presence of the prolines at the dimer interface of WT leads to formation of a lower affinity dimer that is dynamic. This phenomenon was supported by our studies of PPAA, which forms a very stable dimer regardless of the calcium concentration. Hence, our data unequivocally provide evidence for the role of proline residues in the dynamics of monomer–dimer equilibrium. This finding is physiologically relevant because formation of stable dimer is not ideal for plasticity of synapses and the adherens junctions in general. In addition to the control over the dynamics of dimer formation, our data also suggest that the calcium requirement for dimerization is the results of the occurrence of prolines in the  $\beta$ A-strand. In summary, the proline residues act as a switch to control the dynamics of the equilibrium between monomer and dimer which is crucial for the plasticity of synapses.

## ■ ASSOCIATED CONTENT

### ● Supporting Information

Data for the unfolding of isolated EC1 in the presence and absence of calcium and for the reversibility of the unfolding transition of PPAA. This material is available free of charge via the Internet at <http://pubs.acs.org>.

## ■ AUTHOR INFORMATION

### Corresponding Author

\*Phone: 1-662-915-5328; fax: 1-662-915-7300; e-mail: [spedigo@olemiss.edu](mailto:spedigo@olemiss.edu).

## Funding

This work was supported by grant MCB 0950494 from the National Science Foundation.

## ■ ABBREVIATIONS

Apo, calcium-depleted; CD, circular dichroism; EC, extracellular domains; EC1, extracellular domain 1 of NCAD12; EC2, extracellular domain 2 of NCAD12; EGTA, ethylene glycol tetraacetic acid; GHCl, guanidine hydrochloride; HEPES, *N*-(2-hydroxyethyl)piperazine-*N'*-2-ethanesulfonic acid;  $K_d$ , dissociation constant; NCAD12, neural cadherin domains 1 and 2 (residues 1 to 221); PPAA, mutation of prolines 5 and 6 to alanine in NCAD12; PAGE, polyacrylamide gel electrophoresis; SEC, size exclusion chromatography;  $T_m$ , melting temperature; WT, wild-type NCAD12.

## ■ REFERENCES

- (1) Fannon, A. M., and Colman, D. R. (1996) A model for central synaptic junctional complex formation based on the differential adhesive specificities of the cadherins. *Neuron* 17, 423–434.
- (2) Uchida, N., Honjo, Y., Johnson, K. R., Wheelock, M. J., and Takeichi, M. (1996) The catenin/cadherin adhesion system is localized in synaptic junctions bordering transmitter release zones. *J. Cell Biol.* 135, 767–779.
- (3) Jungling, K., Eulenburg, V., Moore, R., Kemler, R., Lessmann, V., and Gottmann, K. (2006) N-cadherin transsynaptically regulates short-term plasticity at glutamatergic synapses in embryonic stem cell-derived neurons. *J. Neurosci.* 26, 6968–6978.
- (4) Huntley, G. W., Gil, O., and Bozdagi, O. (2002) The cadherin family of cell adhesion molecules: multiple roles in synaptic plasticity. *Neuroscientist* 8, 221–233.
- (5) Tang, L., Hung, C. P., and Schuman, E. M. (1998) A role for the cadherin family of cell adhesion molecules in hippocampal long-term potentiation. *Neuron* 20, 1165–1175.
- (6) Harrison, O. J., Jin, X., Hong, S., Bahna, F., Ahlsen, G., Brasch, J., Wu, Y., Vendome, J., Felsovalyi, K., Hampton, C. M., Troyanovsky, R. B., Ben-Shaul, A., Frank, J., Troyanovsky, S. M., Shapiro, L., and Honig, B. (2011) The extracellular architecture of adherens junctions revealed by crystal structures of type I cadherins. *Structure* 19, 244–256.
- (7) Kemler, R., and Ozawa, M. (1989) Uvomorulin-catenin complex: cytoplasmic anchorage of a  $Ca^{2+}$ -dependent cell adhesion molecule. *Bioessays* 11, 88–91.
- (8) Takeichi, M. (1977) Functional correlation between cell adhesive properties and some cell surface proteins. *J. Cell Biol.* 75, 464–474.
- (9) Nose, A., Nagafuchi, A., and Takeichi, M. (1988) Expressed recombinant cadherins mediate cell sorting in model systems. *Cell* 54, 993–1001.
- (10) Pokutta, S., Herrenknecht, K., Kemler, R., and Engel, J. (1994) Conformational changes of the recombinant extracellular domain of E-cadherin upon calcium binding. *Eur. J. Biochem.* 223, 1019–1026.
- (11) Haussinger, D., Ahrens, T., Aberle, T., Engel, J., Stetefeld, J., and Grzesiek, S. (2004) Proteolytic E-cadherin activation followed by solution NMR and X-ray crystallography. *EMBO J.* 23, 1699–1708.
- (12) Boggon, T. J., Murray, J., Chappuis-Flament, S., Wong, E., Gumbiner, B. M., and Shapiro, L. (2002) C-cadherin ectodomain structure and implications for cell adhesion mechanisms. *Science* 296, 1308–1313.
- (13) Parisini, E., Higgins, J. M., Liu, J. H., Brenner, M. B., and Wang, J. H. (2007) The crystal structure of human E-cadherin domains 1 and 2, and comparison with other cadherins in the context of adhesion mechanism. *J. Mol. Biol.* 373, 401–411.
- (14) Fink, A. L. (1998) Protein aggregation: folding aggregates, inclusion bodies and amyloid. *Folding Des.* 3, R9–23.

- (15) Bergdoll, M., Remy, M. H., Cagnon, C., Masson, J. M., and Dumas, P. (1997) Proline-dependent oligomerization with arm exchange. *Structure* 5, 391–401.
- (16) Rousseau, F., Schymkowitz, J. W., Wilkinson, H. R., and Itzhaki, L. S. (2001) Three-dimensional domain swapping in p13suc1 occurs in the unfolded state and is controlled by conserved proline residues. *Proc. Natl. Acad. Sci. U. S. A.* 98, 5596–5601.
- (17) Posy, S., Shapiro, L., and Honig, B. (2008) Sequence and structural determinants of strand swapping in cadherin domains: do all cadherins bind through the same adhesive interface? *J. Mol. Biol.* 378, 954–968.
- (18) Vunnam, N., and Pedigo, S. (2011) Sequential binding of calcium leads to dimerization in neural cadherin. *Biochemistry* 50, 2973–2982.
- (19) Pace, C. N., Vajdos, F., Fee, L., Grimsley, G., and Gray, T. (1995) How to measure and predict the molar extinction coefficient of a protein. *Protein Sci.* 4, 2411–2423.
- (20) Vunnam, N., Flint, J., Balbo, A., Schuck, P., and Pedigo, S. (2011) Dimeric States of Neural- and Epithelial-Cadherins are Distinguished by the Rate of Disassembly. *Biochemistry* 50, 2951–2961.
- (21) Prasad, A., Housley, N. A., and Pedigo, S. (2004) Thermodynamic stability of domain 2 of epithelial cadherin. *Biochemistry* 43, 8055–8066.
- (22) Ando, K., Uemura, K., Kuzuya, A., Maesako, M., Asada-Utsugi, M., Kubota, M., Aoyagi, N., Yoshioka, K., Okawa, K., Inoue, H., Kawamata, J., Shimohama, S., Arai, T., Takahashi, R., and Kinoshita, A. (2011) N-cadherin regulates p38 MAPK signaling via association with JNK-associated leucine zipper protein: implications for neurodegeneration in Alzheimer disease. *J. Biol. Chem.* 286, 7619–7628.
- (23) Prasad, A., and Pedigo, S. (2005) Calcium-dependent Stability Studies of Domains 1 and 2 of Epithelial Cadherin. *Biochemistry* 44, 13692–13701.
- (24) Vendome, J., Posy, S., Jin, X., Bahna, F., Ahlsen, G., Shapiro, L., and Honig, B. (2011) Molecular design principles underlying beta-strand swapping in the adhesive dimerization of cadherins. *Nat. Struct. Mol. Biol.* 18, 693–700.
- (25) De Roo, M., Klauser, P., Garcia, P. M., Poglia, L., and Muller, D. (2008) Spine dynamics and synapse remodeling during LTP and memory processes. *Prog. Brain Res.* 169, 199–207.